

Importance of a finite speed of heat propagation in metals irradiated by femtosecond laser pulses

J. J. Klossika, U. Gratzke, M. Vicanek,* and G. Simon

Institut für Theoretische Physik, Technische Universität, Mendelssohnstrasse 3, D-38106 Braunschweig, Germany

(Received 15 March 1996; revised manuscript received 25 July 1996)

We study theoretically the propagation of heat in a metal, due to irradiation with an ultrashort laser pulse. The target is treated in an extended two-fluid model for electrons and phonons, which accounts for a finite speed of heat propagation in the electron gas. As a result, the absorbed laser energy is more localized in the electronic system yielding an enhanced peak electron temperature. [S0163-1829(96)01431-2]

Laser radiation is absorbed in a metal in three steps: (a) the electrons are accelerated in the electromagnetic field, (b) the electron gas thermalizes via Coulomb collisions on a time scale of about a picosecond. In the last step, (c) the hot electron gas releases its energy to the lattice via electron-phonon collisions on a time scale of a few picoseconds. The time scale for internal thermalization of the electron gas is somewhat shorter than the one for equilibration with the lattice.

The internal electronic relaxation time in a metal has been measured by many authors, see, e.g., Refs. 1–6. In a typical experiment,⁵ an optically thin gold film of 200 Å thickness was irradiated by an infrared laser pulse of 120 fs duration. A laser fluence of the pump pulse of 2.5 . . . 200 μJ/cm⁻² was used. Transient reflection and transmission characteristics were monitored with a probe laser pulse. In their experiments, Sun *et al.*⁵ found an internal electronic relaxation time of 500 fs, independent of the laser fluence.

As already pointed out by Fann *et al.*^{1,2} the electron energy distribution may be decomposed into a thermal and a nonthermal part. Sun *et al.*⁵ calculated the energy dependent relaxation dynamics of the electron distribution. To do so, a simulation based on a numerical solution of the Boltzmann equation was carried out. The transient behavior of reflectivity, transmittivity, and electron occupation number were obtained in good agreement with experimental values.

More recently, Groeneveld *et al.*⁶ set up similar experiments on silver and gold films. In addition to Sun *et al.*, they varied the lattice temperature from 300 K down to 10 K and found a slight decrease in the electron relaxation time.

Besides the temporal aspect, which has been the main focus in these investigations, there is also a spatial aspect to the phenomenon: energy is initially absorbed within a thin surface layer, only to be carried away by electrons in the next instant and spread out over a larger volume. Thus, the interaction of laser pulses with surfaces must be viewed as an interplay between thermalization energy exchange, and transport.

In this paper, we extend Anisimov's⁷ two-fluid model for the electron and phonon systems in a metal by Cattaneo's law for the heat flux to account for a finite propagation speed of heat. A comprehensive review on heat waves was given by Joseph and Preziosi.⁸ The present extension gives some insight into the temporal *and* spatial behavior of electron and phonon temperature; in this respect, the model goes beyond

the kinetic treatment of energy relaxation performed by Sun *et al.*, which is independent of space.

Cattaneo's law⁹ for the heat flux \mathbf{q} in the electron gas reads

$$\tau \frac{\partial \mathbf{q}}{\partial t} + \mathbf{q} = -k_e \text{grad} T_e, \quad (1)$$

where τ is the common electron relaxation time and k_e is the electronic thermal conductivity. Together with energy conservation,

$$\frac{\partial \epsilon}{\partial t} = -\text{div} \mathbf{q}, \quad (2)$$

where ϵ is the internal energy density of the system, we obtain for the electron temperature $T_e(x,t)$ and the phonon temperature $T_p(x,t)$ in the usual one-dimensional description,

$$C_e \frac{\partial T_e}{\partial t} + \tau \frac{\partial}{\partial t} C_e \frac{\partial T_e}{\partial t} = \frac{\partial}{\partial x} k_e \frac{\partial T_e}{\partial x} - G(T_e - T_p) - \tau \frac{\partial}{\partial t} G(T_e - T_p), \quad (3)$$

$$C_p \frac{\partial T_p}{\partial t} = G(T_e - T_p). \quad (4)$$

Equation (3) is a partial differential equation of hyperbolic type. C_e and C_p are the specific heats of electron gas and phonon gas, respectively, and G is the coupling constant between the two systems. The second term of the left-hand side of Eq. (3), $\tau_{ee} \partial/\partial t (C_e \partial T_e/\partial t)$, provides a finite propagation speed $v = \sqrt{k_e/(C_e \tau_{ee})}$ of a heat wave into the material. The magnitude of v is related to the Fermi velocity. The term $\tau_{ee} \partial/\partial t [G(T_e - T_p)]$ accounts for a relaxed energy transfer to phonons, a term which is required from energy conservation. The usual model with parabolic heat conduction in the electronic subsystem is recovered by setting $\tau_{ee} = 0$, i.e., $v \rightarrow \infty$, and will be treated here for comparison.

The material parameters C_e , C_p , G , k_e , and τ_{ee} in Eqs. (3) and (4) are, in general, functions of temperature. We seek analytical solutions and restrict the analysis to small temperature variations, i.e., low pulse energies. Hence the material parameters will be treated as constants.

The penetration depth of UV laser light in metals is of the order of a few nanometers, but will be neglected in the present model. Accordingly, all laser energy is absorbed at the surface ($x=0$) by the electron gas and is converted to a heat flux q . We use a Gaussian pulse,

$$q = Q \exp[-(t-t_0)^2/t_h^2] \text{ for } x=0, \quad t \geq 0, \quad (5)$$

where t_0 is an offset time, t_h denotes the half width, and Q stands for the peak laser intensity. Deep inside ($x \rightarrow \infty$) we assume ambient temperature which, due to linearity, may be chosen as zero.

The system will be solved for an initially ($t=0$) cold target,

$$T_e = T_p = 0, \quad \frac{\partial T_e}{\partial t} = 0 \text{ for } x \geq 0, \quad t = 0. \quad (6)$$

Applying the Laplace transform with respect to time to the system (3, 4), we obtain solutions in terms of x and the transformed coordinate s ,

$$T_e(x,s) = \frac{\sqrt{\pi} Q t_h}{2k_e} \exp\left(\frac{s^2 t_h^2}{4} - s t_0\right) \operatorname{erfc}\left(\frac{s t_h}{2} - \frac{t_0}{t_h}\right) \times \frac{1+s\tau}{r(s)} e^{-xr(s)}, \quad (7)$$

$$T_p(x,s) = \frac{T_e(x,s)}{1 + C_p s/G}. \quad (8)$$

In Eq. (7), $\operatorname{erfc}(x)$ denotes the complementary error function, and $r(s)$ is given by

$$r(s) = \left[\frac{C_e + C_p}{k_e} \frac{s(1+s\tau)(1+s\tau_{ep})}{1 + C_p s/G} \right]^{1/2}, \quad (9)$$

where

$$\tau_{ep} = \frac{C_e C_p}{(C_e + C_p)G} \quad (10)$$

is the electron-phonon energy relaxation time. Inversion of the above expressions is accomplished numerically using the method by Honig and Hirdes.¹⁰

We present a typical result for gold as target material and use a pulse of $2t_h=30$ fs duration, $t_0=45$ fs, with a maximum intensity of $Q=1.25 \times 10^{11} \text{ W m}^{-2}$. The following parameters for gold were used:¹¹ electronic specific heat $C_e=2.1 \times 10^4 \text{ J m}^{-3} \text{ K}^{-1}$, corresponding to the value at 300 K, electronic thermal conductivity $k_e=315 \text{ W m}^{-1} \text{ K}^{-1}$, lattice specific heat $C_p=2.5 \times 10^6 \text{ J m}^{-3} \text{ K}^{-1}$, and coupling constant $G=3.5 \times 10^{16} \text{ W m}^{-3} \text{ K}^{-1}$. For the electronic relaxation time, we took $t=30$ fs from Ref. 12.

Due to the finite propagation speed, heat penetrates in form of temperature waves into the material. In Fig. 1(a), the transient behavior of the electron temperature at a depth $x=50$ nm is shown (full curve) in comparison to the usual model (dotted curve) with $\tau=0$ in Eq. (3). Clearly, the usual and the extended model give quite different results. The electron temperature rises more rapidly and attains a maximum value that is 2.5 times as high as compared to the case with

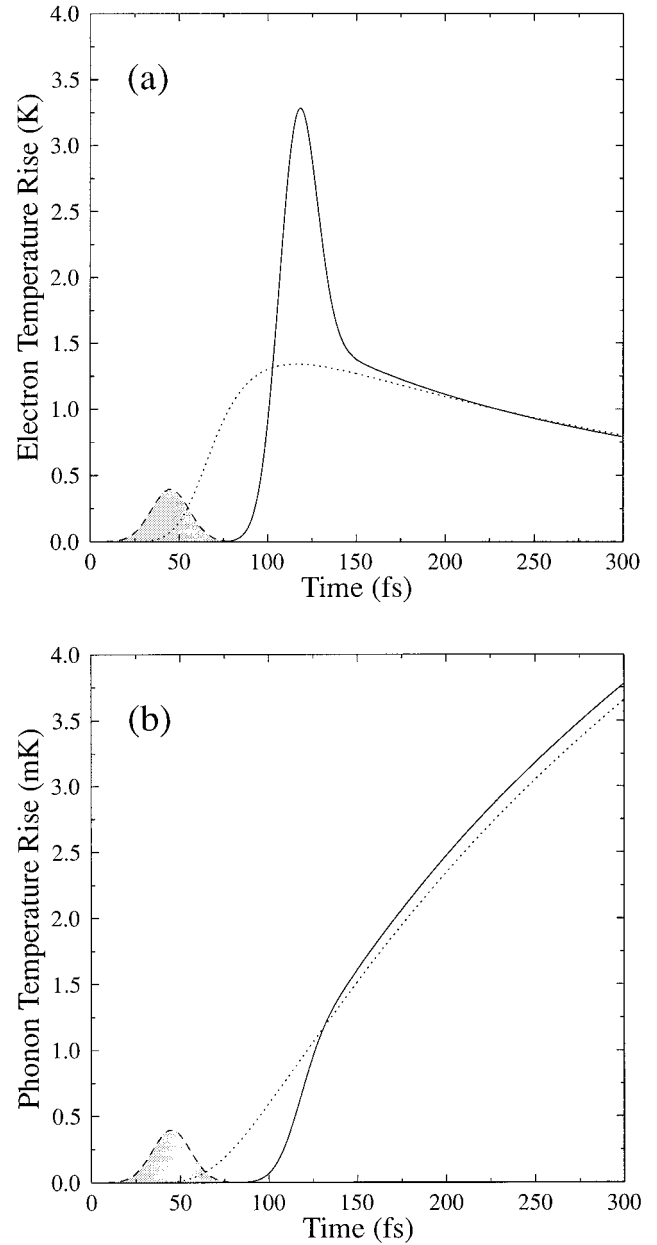


FIG. 1. Transient behavior of electron temperature (a) and phonon temperature (b). The solid curve and the dotted curve refer to a model with finite and infinite heat propagation speed, respectively. The laser pulse centered at 180 fs is displayed as a point of reference.

infinite propagation speed. The heating rate of the phonon gas, see Fig. 1(b) rises by about the same.

The spatial behavior of the electronic temperature wave at a time $t=118$ fs is illustrated in Fig. 2. In the extended model (full line), the energy is peaked in a small region of approximately 30 nm. This is drastically different from the model with infinite propagation speed (dotted line), which predicts a much shallower and essentially structureless temperature profile.

We will now give a critical discussion of the model and the physical input used. The value of the coupling constant G is not accurately known. Experimental results for gold reach from $3.5 \times 10^{16} \text{ W m}^{-3} \text{ K}^{-1}$ (Ref. 11) to 2.7×10^{17}

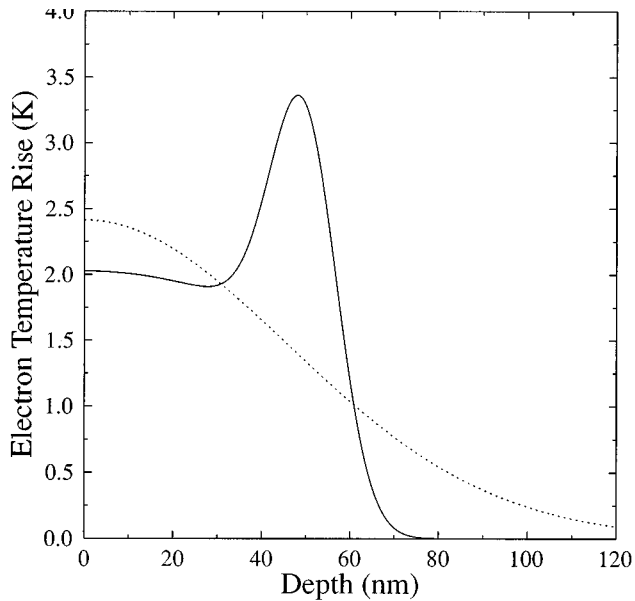


FIG. 2. Spatial behavior of the electronic temperature wave at a time $t = 750$ fs. Full curve: present model with finite propagation speed. Dotted curve: conventional model with infinite propagation speed.

$\text{Wm}^{-3} \text{K}^{-1}$.¹³ Usually, G is fitted to experimental data on the basis of the common two-fluid model, even when femto-second laser pulses are used, see, e.g., Orlande.¹⁴ The exact dependence of G on electron temperature is unknown; Allen¹⁵ gives an expression $\propto T_e^n$, with $1 < n < 3$, while Girardeau-Montaut and Girardeau-Montaut¹³ propose $G \propto T_e^{1/2}$.

The temperature dependence of material parameters results, in principle, in a nonlinear system (3,4). When higher laser intensities are applied, e.g., for ablation^{16,17} of metals,

the linear approximation used here breaks down, and the full temperature dependencies of electronic heat capacity and electron-phonon coupling have to be taken into account. Qualitatively, this will lead to a sublinear increase of electron temperature with laser intensity.

A finite skin depth was neglected in the present model. For UV lasers irradiating gold, its value is of the order of a few nanometers, the results given here refer to a depth of 50 nm, where this simplification is justified. Inclusion of a finite skin depth is straightforward in the present scheme and could be carried out when shallower depths are of concern, e.g., in the context of ablation.

The value for the speed of heat propagation $v = 7 \times 10^5$ m/s used in our calculation is by and large consistent with measurements of heat transport velocity in thin gold films by Brorson *et al.*¹⁸ They found heat propagating at speeds of the order of Fermi velocity 10^6 m/s.

The concept of an electron temperature needs careful inspection in situations when the electron gas is not in thermal equilibrium. More detailed studies^{2,5} suggest that the electron energy distribution could be decomposed into a thermal and a nonthermal, energetic part. Whether or not the system may be described by a single *effective* temperature depends on the quantity considered. Such a simplified picture appears adequate for energy deposition dynamics as such. Caution is indicated, however, when threshold effects come into play. Electron emission, for instance, is sensitive only to the high-energy part of the spectrum.

To conclude, we extended the two-fluid model for electrons and phonons in a metal by introducing a finite speed of heat propagation. When a metallic surface is exposed to a laser pulse, peak electron temperatures may attain values considerably higher compared to the usual model. Likewise, the lattice heating rate may be much higher.

We thank S. I. Anisimov and B. Rethfeld for clarifying discussions.

*Electronic address: M.Vicanek@tu-bs.de

¹W. S. Fann, R. Storz, H. W. K. Tom, and J. Bokor, Phys. Rev. Lett. **68**, 2834 (1992).

²W. S. Fann, R. Storz, H. W. K. Tom, and J. Bokor, Phys. Rev. B **46**, 13 592 (1992).

³R. H. M. Groeneveld, R. Sprik, and A. Lagendijk, Phys. Rev. B **45**, 5079 (1992).

⁴C.-K. Sun, F. Vallée, L. Acioli, E. P. Ippen, and J. G. Fujimoto, Phys. Rev. B **48**, 12 365 (1993).

⁵C.-K. Sun, F. Vallée, L. H. Acioli, E. P. Ippen, and J. G. Fujimoto, Phys. Rev. B **50**, 15 337 (1994).

⁶R. H. M. Groeneveld, R. Sprik, and A. Lagendijk, Phys. Rev. B **51**, 11 433 (1995).

⁷S. I. Anisimov, B. L. Kapeliovich, and T. L. Perel'man, Zh. Éksp. Teor. Fiz. **66**, 776 (1974) [Sov. Phys. JETP **39**, 375 (1974)].

⁸D. D. Joseph and L. Preziosi, Rev. Mod. Phys. **61**, 41 (1989); **62**, 375 (1990).

⁹C. Cattaneo, Atti Semin. Mat. Fis. Univ. Modena **3**, 3 (1948); C.

Cattaneo, R. C. Acad. Sci. **247**, 431 (1958).

¹⁰G. Honig and U. Hirdes, Ber. Kernforschungsanlage Jülich No. 1672 (1979).

¹¹X. Y. Wang, D. M. Riffe, Y.-S. Lee, and M. C. Downer, Phys. Rev. B **50**, 8016 (1994).

¹²N. W. Ashcroft and N. D. Mermin, *Solid State Physics* (Saunders College, Fort Worth, 1976).

¹³J. P. Girardeau-Montaut and C. Girardeau-Montaut, Phys. Rev. B **51**, 13 560 (1995).

¹⁴H. R. B. Orlande, M. N. Özisik, and D. Y. Tzou, J. Appl. Phys. **78**, 1843 (1995).

¹⁵P. B. Allen, Phys. Rev. Lett. **59**, 1460 (1987).

¹⁶S. Preuss, A. Demchuk, and M. Stuke, Appl. Phys. A **61**, 33 (1995).

¹⁷P. P. Pronko, S. K. Dutta, J. Squier, J. V. Rudd, D. Du, and G. Mourou, Opt. Commun. **114**, 106 (1995).

¹⁸S. D. Brorson, J. G. Fujimoto, and E. P. Ippen, Phys. Rev. Lett. **59**, 1962 (1987).